References

Abbaszade I, Liu RQ, Yang F, Rosenfeld SA, Ross OH, Link JR, Ellis DM, Tortorella MD, Pratta MA, Hollis JM, Wynn R, Duke JL, George HJ, Hillman MC Jr, Murphy K, Wiswall BH, Copeland RA, Decicco CP, Bruckner R, Nagase H, Itoh Y, Newton RC, Magolda RL, Trzaskos JM, Burn TC et al (1999) Cloning and characterization of ADAMTS11, an aggrecanase from the ADAMTS family. J Biol Chem 274:23443–23450

Arner EC (2002) Aggrecanase-mediated cartilage degradation. Curr Opin Pharmacol 2:322–329

Arner EC, Pratta MA, Trzaskos JM, Decicco CP, Tortorella MD (1999) Generation and characterization of aggrecanase. A soluble, cartilage-derived aggrecan-degrading activity. J Biol Chem 274:6594–6601

Bae JW, Takahashi I, Sasano Y, Onodera K, Mitani H, Kagayama M, Mitani H (2003) Age-related changes in gene expression patterns of matrix metalloproteinases and their collagenous substrates in mandibular condylar cartilage in rats. J Anat 203:235–241

Caterson B, Flannery CR, Hughes CE, Little CB (2000) Mechanisms involved in cartilage proteoglycan catabolism. Matrix Biol 19:333–344

Doege KJ, Sasaki M, Kimura T, Yamada Y (1991) Complete coding sequence and deduced primary structure of the human cartilage large aggregating proteoglycan, aggrecan. Human-specific repeats, and additional alternatively spliced forms. J Biol Chem 266:894–902

Fosang AJ, Last K, Maciewicz RA (1996) Aggrecan is degraded by matrix metalloproteinases in human arthritis. Evidence that matrix metalloproteinase and aggrecanase activities can be independent. J Clin Invest 98:2292–2299

Gepstein A, Arbel G, Blumenfeld I, Peled M, Livne E (2003) Association of metalloproteinases, tissue inhibitors of matrix metalloproteinases, and proteoglycans with development, aging, and osteoarthritis processes in mouse temporomandibular joint. Histochem Cell Biol 120:23–32

Glasson SS, Askew R, Sheppard B, Carito B, Blanchet T, Ma HL, Flannery CR, Peluso D, Kanki K, Yang Z, Majumdar MK, Morris EA (2005) Deletion of active ADAMTS5 prevents cartilage degradation in a murine model of osteoarthritis. Nature 434:644–648

Kuno K, Okada Y, Kawashima H, Nakamura H, Miyasaka M, Ohno H, Matsushima K (2000) ADAMTS-1 cleaves a cartilage proteoglycan, aggrecan. FEBS Lett 478:241–245

Lark MW, Bayne EK, Flanagan J, Harper CF, Hoerrner LA, Hutchinson NI, Singer II, Donatelli SA, Weidner JR, Williams HR, Mumford RA, Lohmander LS (1997) Aggrecan degradation in human cartilage. Evidence for both matrix metalloproteinase and aggrecanase activity in normal, osteoarthritic, and rheumatoid joints. J Clin Invest 100:93–106

Lohmander LS, Neame PJ, Sandy JD (1993) The structure of aggrecan fragments in human synovial fluid. Evidence that aggrecanase mediates cartilage degradation in inflammatory joint disease, joint injury, and osteoarthritis. Arthritis Rheum 36:1214–1222

Luder HU, Leblond CP, von der Mark K (1988) Cellular stages in cartilage formation as revealed by morphometry, radioautography and type II collagen immunostaining of the mandibular condyle from weanling rats. Am J Anat 182:197–214

Matthews RT, Gary SC, Zerillo C, Pratta M, Solomon K, Arner EC, Hockfield S (2000) Brain-enriched hyaluronan binding (BEHAB)/brevican cleavage in a glioma cell line is mediated by a disintegrin and metalloproteinase with thrombospondin motifs (ADAMTS) family member. J Biol Chem 275:22695–22703

Mizoguchi I, Nakamura M, Takahashi I, Kagayama M, Mitani H (1992) A comparison of the immunohistochemical localization of type I and type II collagens in craniofacial cartilages of the rat. Acta Anat 144:59–64

Nakamura H, Fujii Y, Inoki I, Sugimoto K, Tanzawa K, Matsuki H, Miura R, Yamaguchi Y, Okada Y (2000) Brevican is degraded by matrix metalloproteinases and aggrecanase-1 (ADAMTS4) at different sites. J Biol Chem 275:38885–38890

Nakamura M, Sone S, Takahashi I, Mizoguchi I, Echigo S, Sasano Y (2005) Expression of versican and ADAMTS1, 4, and 5 during bone development in the rat mandible and hind limb. J Histochem Cytochem 53:1553–1562

Ohashi N, Ejiri S, Hanada K, Ozawa H (1997) Change in type I, II, and X collagen immunoreactivity of the mandibular condylar cartilage in a naturally aging rat model. J Bone Miner Metab 15:77–83

Ohtani H, Kuroiwa A, Obinata M, Ooshima A, Nagura H (1992) Identification of type I collagen-producing cells in human gastrointestinal carcinomas by non-radioactive in situ hybridization and immunoelectron microscopy. J Histochem Cytochem 40:1139–1146

Sandy JD, Verscharen C (2001). Analysis of aggrecan in human knee cartilage and synovial fluid indicates that aggrecanase (ADAMTS) activity is responsible for the catabolic turnover and loss of whole aggrecan whereas other protease activity is required for C-terminal processing in vivo. Biochem J 358:615–626

Sasano Y, Furusawa M, Ohtani H, Mizoguchi I, Takahashi I, Kagayama M (1996) Chondrocytes synthesize type I collagen and accumulate the protein in the matrix during development of rat tibial articular cartilage. Anat Embryol 194:247–252

Shibata S, Fukada K, Suzuki S, Ogawa T, Yamashita Y (2001) Histochemical localization of versican, aggrecan and hyaluronan in the developing condylar cartilage of the fetal rat mandible. J Anat 198:129–135

Silbermann M, Reddi AH, Hand AR, Leapman RD, von der Mark K, Franzen A (1987) Further characterization of the extracellular matrix in the mandibular condyle in neonatal mice. J Anat 151:169–188

Stanton H, Rogerson FM, East CJ, Golub SB, Lawlor KE, Meeker CT, Little CB, Last K, Farmer PJ, Campbell IK, Fourie AM, Fosang AJ (2005) ADAMTS5 is the major aggrecanase in mouse cartilage in vivo and in vitro. Nature 434:648–652

Sztrolovics R, Grover J, Cs-Szabo G, Shi SL, Zhang Y, Mort JS, Roughley PJ (2002) The characterization of versican and its message in human articular cartilage and intervertebral disc. J Orthop Res 20:257–266

Takahashi I, Mizoguchi I, Sasano Y, Saitoh S, Ishida M, Kagayama M, Mitnai H (1996) Age-related changes in the localization of glycosaminoglycans in condylar cartilage of the mandible in rats. Anat Embryol 194:489–500

Tang BL (2001) ADAMTS: a novel family of extracellular matrix proteases. Int J Biochem Cell Biol 33:33–44

Ten Cate AR (1994) Temporomandibular joint In: Ten Cate AR (ed) Oral histology: development, structure, and function, 4th edn. Mosby, St. Louis, pp 432–455

Tortorella MD, Burn TC, Pratta MA, Abbaszade I, Hollis JM, Liu R, Rosenfeld SA, Copeland RA, Decicco CP, Wynn R, Rockwell A, Yang F, Duke JL, Solomon K, George H, Bruckner R, Nagase H, Itoh Y, Ellis DM, Ross H, Wiswall BH, Murphy K, Hillman MC Jr, Hollis GF, Newton RC, Magolda RL, Trzaskos JM, Arner EC (1999) Purification and cloning of aggrecanase-1: a member of the ADAMTS family of proteins. Science 284:1664–1666

Tortorella M, Pratta M, Liu RQ, Abbaszade I, Ross H, Burn T, Arner E (2000) The thrombospondin motif of aggrecanase-1 (ADAMTS-4) is critical for aggrecan substrate recognition and cleavage. J Biol Chem 275:25791–25797

Zhu JX, Sasano Y, Takahashi I, Mizoguchi I, Kagayama M (2001) Temporal and spatial gene expression of major bone extracellular matrix molecules during embryonic mandibular osteogenesis in rats. Histochem J 33:25–35

RESEARCH REPORTS
Biological

L. Liu[1,4], K. Igarashi[2]*, H. Kanzaki[1], M. Chiba[2], H. Shinoda[3], and H. Mitani[1]

Divisions of [1]Orthodontics and Dentofacial Orthopedics, [2]Oral Dysfunction Science, and [3]Dental Pharmacology, Department of Oral Health and Development Sciences, Tohoku University Graduate School of Dentistry, 4-1 Seiryo-machi, Aoba-ku, Sendai 980-8575, Japan; [4]present address, Department of Orthodontics, Dalian University Stomatology Hospital, Dalian, China; *corresponding author, igarashi@mail.tains.tohoku.ac.jp

J Dent Res 85(8):757-760, 2006

Clodronate Inhibits PGE_2 Production in Compressed Periodontal Ligament Cells

ABSTRACT

Periodontal ligament (PDL) cells play an essential role in orthodontic tooth movement. We recently reported that clodronate, a non-N-containing bisphosphonate, strongly inhibited tooth movement in rats, and thus could be a useful adjunct for orthodontic treatment. However, it is not clear how clodronate affects the responses of PDL cells to orthodontic force. In this study, we hypothesized that clodronate prevents the mechanical stress-induced production of prostaglandin E_2 (PGE_2), interleukin-1β (IL-1β), and nitric oxide (NO) in human PDL cells. A compressive stimulus caused a striking increase in PGE_2 production, while the responses of IL-1β and NO were less marked. Clodronate concentration dependently inhibited the stress-induced production of PGE_2. Clodronate also strongly inhibited stress-induced gene expression for COX-2 and RANKL. These results suggest that the inhibitory effects of clodronate on tooth movement and osteoclasts may be due, at least in part, to the inhibition of COX-2-dependent PGE_2 production and RANKL expression in PDL cells.

KEY WORDS: clodronate, periodontal ligament cell, mechanical stress, prostaglandin E_2.

Received August 8, 2005; Last revision April 23, 2006; Accepted May 3, 2006

INTRODUCTION

Periodontal ligament cells play an essential role in orthodontic tooth movement, and mechanically induced bone resorption is known to be a rate-limiting step (Rygh, 1987; Igarashi *et al.*, 1994). Recently, we demonstrated that clodronate, a non-N-containing bisphosphonate that has been used to treat various metabolic bone diseases associated with excessive bone resorption (Plosker and Goa, 1994; Fleisch, 2000), strongly inhibited bone resorption induced by orthodontic mechanical stress and tooth movement in rats, suggesting that it could be a useful adjunct for orthodontic treatment (Liu *et al.*, 2004). A previous study has demonstrated the direct inhibitory action of clodronate on osteoclastic bone resorption, *i.e.*, clodronate induces apoptosis of osteoclasts through incorporation into the cells (Frith *et al.*, 2001). Although the number of osteoclasts on the pressure side of the periodontal ligament decreased in clodronate-treated animals, the mechanism of action in this process has not yet been determined. The purpose of the present study was to clarify how clodronate affects the responses of periodontal ligament cells to orthodontic force, especially those leading to bone resorption. In this study, we hypothesized that clodronate prevents the mechanical stress-induced production of prostaglandin E_2 (PGE_2), interleukin 1β (IL-1β), and nitric oxide (NO) in cultured human periodontal ligament cells, which are known to play important roles in the bone-resorptive responses to orthodontic mechanical stimulation (Yamasaki *et al.*, 1980; Chumbley and Tuncay, 1986; Saito *et al.*, 1991; Zhou *et al.*, 1997; Alhashimi *et al.*, 2001; Iwasaki *et al.*, 2001; Hayashi *et al.*, 2002; Shirazi *et al.*, 2002).

MATERIALS & METHODS

The protocol for the experiment was approved by the Research Ethics Committee of Tohoku University Graduate School of Dentistry, and informed consent was obtained from all patients.

Drug

Clodronate (dichloromethylene bisphosphonate disodium salts) was obtained from Procter & Gamble Pharmaceuticals' Woods Corners Laboratories (Norwich, NY, USA).

Compression of Primary Human Periodontal Ligament Cells

Primary periodontal ligament cells were derived from human tooth roots extracted for orthodontic treatment. Donors were healthy young adults of both sexes (from 20 to 34 yrs old), free of periodontal disease. The cells were cultured in α-MEM supplemented with 10% FBS, antibiotics, and 1×10^{-8} M 1α,25-dihydroxyvitamin D_3 (Duphar, Amsterdam, Netherlands) at 37°C in an atmosphere of 5% CO_2 in humidified air. The medium was changed every 5 days, and the cells underwent from 4 to 8 passages until use.

For the experiment, periodontal ligament cells were seeded on 35-mm wells in a six-well plate at a density of 3×10^5 cells/dish and cultured until they were confluent. They were then transferred to 2 mL of fresh medium that contained a specific concentration of clodronate and cultured for an additional 24 hrs. After

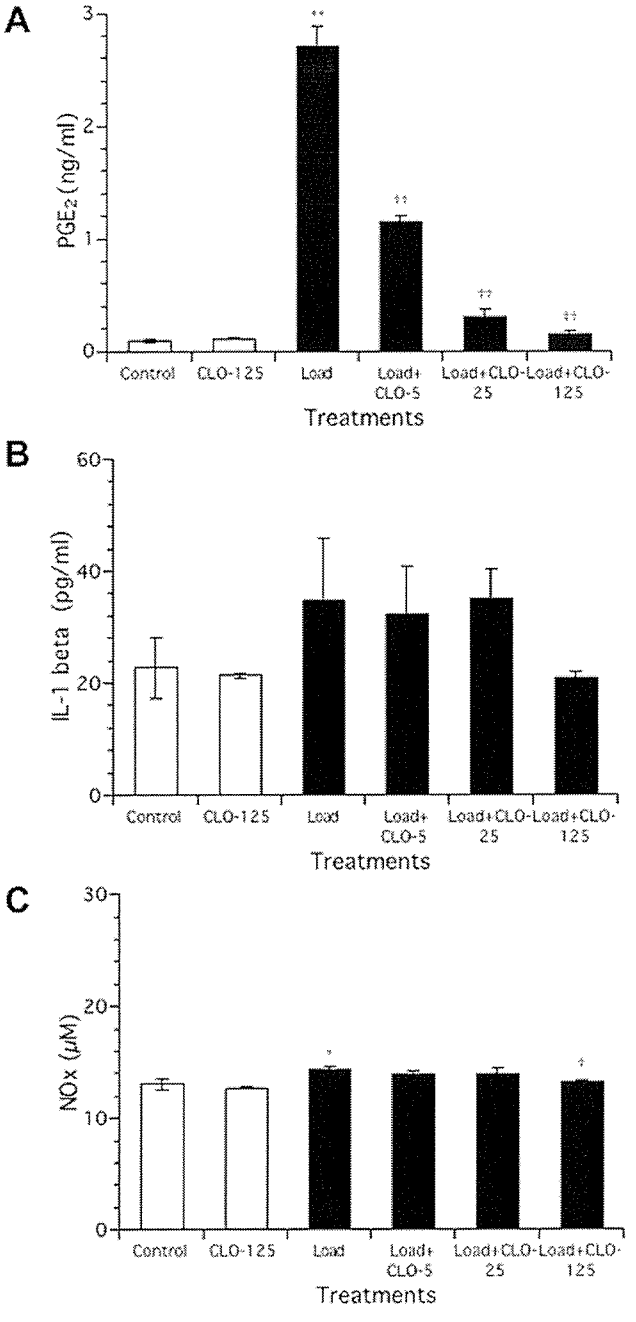

Figure 1. Effects of clodronate on prostaglandin E_2 (PGE_2) (**A**), interleukin 1β (IL-1β) (**B**), and nitric oxide (NO) (**C**) production in periodontal ligament cells induced by compressive mechanical stress. Each column and bar represent the mean ± SEM (n = 3). *Significant increase *vs.* control ($P < 0.05$). **Significant increase *vs.* control ($P < 0.01$). $^{\dagger}P < 0.05$ compared with load. $^{\dagger\dagger}P < 0.01$ compared with load. CLO: clodronate (5, 25, 125 μM).

the pre-culture, the cells were continuously compressed according to the method described previously (Kanzaki *et al.*, 2002). Briefly, compressive force was applied directly to periodontal ligament cells by the placement of a custom-made glass cylinder (diameter, 30.3 mm; height, 14.8 mm; thickness, 2.0 mm) that contained lead granules over a confluent cell layer in the well. We adjusted the force magnitude by adding or reducing the granules. In the present study, the cells were subjected to 2.0 g/cm^2 of compressive force for 48 hrs. After the experiment, total RNA was extracted from each culture with the use of the QuickPrep Total RNA Extraction Kit (Pharmacia Biotech, Uppsala, Sweden). The culture medium was also withdrawn and stored at -20°C for determination of PGE_2, IL-1β, and NO. The concentrations of PGE_2 and IL-1β were measured with respective specific enzyme immunoassay kits (for PGE_2, RPN222, Amersham Pharmacia Biotech, Little Chalfont, Buckinghamshire, UK; for IL-1β, QLB00, R&D Systems, Inc., Minneapolis, MN, USA).(**AQ**) We evaluated NO production by measuring nitrite and nitrate concentrations in the medium using the HPLC-Griess method (Ohta *et al.*, 1994).

Since responsiveness of cultured human periodontal ligament cells varies depending on their sources, the experiment was repeated, and each single experiment was performed with cells from a different subject.

Semi-quantitative Reverse-transcription Polymerase Chain-reaction (RT-PCR) Assays for Cyclo-oxygenase-2 (COX-2) and Receptor Activator Nuclear Factor κB Ligand (RANKL) Gene Expression

We reverse-transcribed extracted RNA to synthesize cDNA using You-Prime First Strand Beads (Pharmacia Biotech) and Oligo $(dT)_{15}$ primer (Promega, Madison, WI, USA). First-strand cDNA was then subjected to PCR amplification with gene-specific PCR primers. The primers used in this study were: 5′-AGC AGA GAA AGC GAT GGT-3′ (forward) and 5′-GGG TAT GAG AAC TTG GGA TT-3′ (reverse) for RANKL, 5′-AAC CCA CTC CAA ACA CAG-3′ (forward) and 5′-CTG GCC CTC GCT TAT GAT CT-3′ (reverse) for COX-2, and 5′-ATG AGG ATC CTC ACC GAG CGC GGC TAC AGC-3′ (forward) and 5′-ACA CCA CTG TGT TGG CGT ACA GGT CTT TGC-3′ (reverse) for β-actin. PCR was performed with a KOD Dash DNA Polymerase Kit (Toyobo Co., Ltd.; LDP-101, Tokyo, Japan). Annealing temperatures were 58°C for RANKL, 51°C for COX-2, and 58°C for β-actin. Numbers of PCR cycles were 42-44 for RANKL, 32-33 for COX-2, and 27 for β-actin. The PCR products were subjected to electrophoresis and stained with ethidium bromide. The relative intensities of the gel bands were measured with the use of Scion Image Analysis software (Scion Co., MD).(**AQ**) The method has been described in detail previously (Kanzaki *et al.*, 2002).

Statistical Analysis

The data were subjected to one-way analysis of variance (ANOVA), followed by Fisher's PLSD test. $P < 0.05$ was considered a significant difference.

RESULTS

Clodronate showed different effects on PGE_2, IL-1β, and NO production in periodontal ligament cells induced by compressive mechanical stress (Fig. 1). The compression of cells at 2.0 g/cm^2 for 48 hrs caused nearly a 30-fold increase in PGE_2 release (Fig. 1A), while the increase was not significant for IL-1β (Fig. 1B) and only minimal for NO (Fig. 1C). Clodronate (5, 25, 125 μM) concentration-dependently inhibited the mechanical stress-induced increase in PGE_2 production in periodontal ligament cells (Fig. 1A). The inhibitory effect of clodronate on NO production was significant only at the highest concentration (125 μM) (Fig. 1C).

The application of compressive force to periodontal ligament cells also caused a more than two-fold increase in

mRNA expression for both COX-2 and RANKL (Figs. 2A, 2B). Clodronate (5, 25, 125 μM) significantly inhibited these responses (Fig. 2B).

Although the responsiveness of periodontal ligament cells to compression varied between and among experiments (individuals), the inhibitory effects of clodronate on stress-induced PGE_2, COX-2, and RANKL were reproducible (Table).

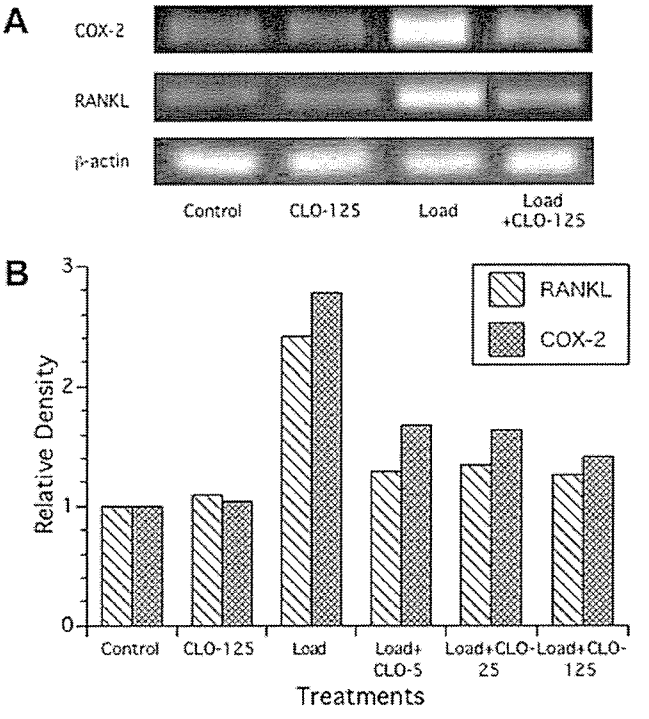

Figure 2. Effect of clodronate on gene expression for cyclo-oxygenase-2 (COX-2) and receptor activator nuclear factor κB ligand (RANKL) in compressed periodontal ligament cells. **(A)** RT-PCR for COX-2, RANKL, and β-actin. CLO: 125 μM. **(B)** Relative expression of RANKL mRNA and COX-2 mRNA determined by densitometric analysis. Values were corrected for β-actin mRNA expression. Representative results of 1 of 3 independent experiments are shown. CLO: clodronate (5, 25, 125 μM).

DISCUSSION

Clodronate is a non-N-containing bisphosphonate that possesses potential anti-inflammatory activity as well as anti-bone-resorptive activity (Österman *et al.*, 1995; Richards *et al.*, 2001). It has been shown that clodronate inhibits the production of pro-inflammatory molecules, including IL-1β (Pennanen *et al.*, 1995; Makkönen *et al.*, 1999), NO (Makkönen *et al.*, 1996; 1999), and PGE_2 (Felix *et al.*, 1981; Igarashi *et al.*, 1997) in macrophages and/or osteoblastic cells.

The present results clearly demonstrated that clodronate could also prevent the mechanical stress-induced production of PGE_2 by periodontal ligament cells, which is one of the most important signaling molecules in the responses of periodontal ligament to orthodontic force (Yamasaki *et al.*, 1980; Saito *et al.*, 1991; Kanzaki *et al.*, 2002). The compressive stimulus caused a striking increase in PGE_2 production, while responses were less marked for IL-1β and NO. Clodronate significantly inhibited the mechanical stress-induced production of PGE_2 in a concentration-dependent manner. Furthermore, clodronate strongly inhibited stress-induced gene expression for COX-2 and RANKL.

Prostaglandins have been shown to play a crucial role in osteoclast formation induced by orthodontic mechanical stress (Yamasaki *et al.*, 1980; Sandy and Harris, 1984; Zhou *et al.*, 1997). Recently, Kanzaki *et al.* (2002) demonstrated that compressive force stimulates osteoclastogenesis in the co-culture of peripheral blood mononuclear cells with periodontal ligament cells, by increasing the expression of RANKL in periodontal ligament cells. RANKL is known to be an essential factor in the differentiation and activation of osteoclasts (Suda *et al.*, 1999). It has also been demonstrated that this increase in RANKL expression paralleled that in COX-2 expression and was dependent on PGE_2 production (Kanzaki *et al.*, 2002). Clodronate inhibited all of these responses in compressed periodontal ligament cells, suggesting that it may have decreased RANKL expression in these cells by inhibiting the COX-2-dependent production of PGE_2. At present, the mechanism by which clodronate inhibits COX-2 expression in periodontal ligament cells is not known. Although NO and IL-1 have been shown to induce COX-2 in osteoblastic cells (Buttery *et al.*, 2002; Pilbeam *et al.*, 2002), their involvement is not likely, since the effects of mechanical stress with or without clodronate on the production of these molecules were only minimal or insignificant.

In our previous *in vivo* study, the number of osteoclasts on the pressure side of the periodontal ligament decreased in clodronate-injected animals (Liu *et al.*, 2004), indicating that clodronate may have either inhibited the recruitment of osteoclasts, promoted osteoclast apoptosis, or both (Rogers *et al.*, 2000). The present *in vitro* results suggest that clodronate may have impaired the ability of periodontal ligament cells to support osteoclast formation by decreasing RANKL expression. It is also possible that the decreased expression of RANKL promoted osteoclast apoptosis, and hence decreased the number of osteoclasts, since RANKL has been shown to act as a survival factor and to prevent apoptosis of osteoclasts (Lacey *et al.*, 2000). Osteoclast apoptosis has been considered to be a major

Table. Comparison of the Effects of Clodronate on Stress-induced Prostaglandin E_2 (PGE_2), Cyclo-oxygenase-2 (COX-2), and Receptor Activator Nuclear Factor κB Ligand (RANKL) in Human Periodontal Ligament Cells among Experiments (individuals)

Variables	Experiment[a]	Treatments: Control	Load	Load ± Clodronate (25 μM)
PGE_2 (ng/mL)	1	0.09 ± 0.02	2.70 ± 0.18	0.29 ± 0.07
	2	0.12 ± 0.01	0.45 ± 0.04	0.20 ± 0.05
COX-2 mRNA (Relative expression)	1	1.00	2.78	1.64
	2	1.00	3.32	2.07
RANKL mRNA (Relative expression)	1	1.00	2.42	1.34
	2	1.00	3.21	2.19

[a] Each experiment was performed with cells from a different individual.

mechanism of action for the inhibition of bone resorption by this bisphosphonate (Halasy-Nagy *et al.*, 2001). Frith *et al.* (2001) demonstrated that clodronate is incorporated into osteoclasts and metabolized to adenosine 5′-(β, γ-dichloromethylene) triphosphate, which may induce apoptosis in these cells. In addition to the formation of this ATP analogue, the inhibition of RANKL expression in supporting cells like periodontal ligament cells might also be involved in the induction of apoptosis in osteoclasts.

In conclusion, the present results suggest that the inhibitory effects of clodronate on orthodontic tooth movement and osteoclasts may be due in part to the inhibition of COX-2-dependent PGE_2 production, which leads to decreased RANKL expression in periodontal ligament cells subjected to orthodontic mechanical stress.

ACKNOWLEDGMENTS

This research was supported by a Grant-in-Aid for Scientific Research (C) from the Ministry of Education, Science, Sports, and Culture of Japan (No. 13672138).

REFERENCES

Alhashimi N, Frithiof L, Brudvik P, Bakhiet M (2001). Orthodontic tooth movement and *de novo* synthesis of proinflammatory cytokines. *Am J Orthod Dentofacial Orthop* 119:307-312.

Buttery LDK, Mancini L, Moradi-Bidhendi N, O'Shaughnessy MC, Polak JM, MacIntyre I (2002). Nitric oxide and other vasoactive agents. In: Principles of bone biology. 2nd ed. Vol. 2. Bilezikian JP, Raisz LG, Rodan GA, editors. San Diego: Academic Press, pp. 995-1013.

Chumbley AB, Tuncay OC (1986). The effect of indomethacin (an aspirin-like drug) on the rate of orthodontic tooth movement. *Am J Orthod* 89:312-314.

Felix R, Bettex JD, Fleisch H (1981). Effect of diphosphonates on the synthesis of prostaglandins in cultured calvaria cells. *Calcif Tissue Int* 33:549-552.

Fleisch H (2000). Bisphosphonates in bone disease: from the laboratory to the patient. 4th ed. San Diego: Academic Press, pp. 40-41.

Frith JC, Mönkkönen J, Auriola S, Mönkkönen H, Rogers MJ (2001). The molecular mechanism of action of the antiresorptive and antiinflammatory drug clodronate: evidence for the formation in vivo of a metabolite that inhibits bone resorption and causes osteoclast and macrophage apoptosis. *Arthritis Rheum* 44:2201-2210.

Halasy-Nagy JM, Rodan GA, Reszka AA (2001). Inhibition of bone resorption by alendronate and risedronate does not require osteoclast apoptosis. *Bone* 29:553-559.

Hayashi K, Igarashi K, Miyoshi K, Shinoda H, Mitani H (2002). Involvement of nitric oxide in orthodontic tooth movement in rats. *Am J Orthod Dentofacial Orthop* 122:306-309.

Igarashi K, Mitani H, Adachi H, Shinoda H (1994). Anchorage and retentive effects of a bisphosphonate (AHBuBP) on tooth movements in rats. *Am J Orthod Dentofacial Orthop* 106:279-289.

Igarashi K, Hirafuji M, Adachi H, Shinoda H, Mitani H (1997). Effects of bisphosphonates on alkaline phosphatase activity, mineralization, and prostaglandin E2 synthesis in the clonal osteoblast-like cell line MC3T3-E1. *Prostaglandins Leukot Essent Fatty Acids* 56:121-125.

Iwasaki LR, Haack JE, Nickel JC, Reinhardt RA, Petro TM (2001). Human interleukin-1 beta and interleukin-1 receptor antagonist secretion and velocity of tooth movement. *Arch Oral Biol* 46:185-189.

Kanzaki H, Chiba M, Shimizu Y, Mitani H (2002). Periodontal ligament cells under mechanical stress induce osteoclastogenesis by receptor activator of nuclear factor kappaB ligand up-regulation *via* prostaglandin E2 synthesis. *J Bone Miner Res* 17:210-220.

Lacey DL, Tan HL, Lu J, Kaufman S, Van G, Qiu W, *et al.* (2000). Osteoprotegerin ligand modulates murine osteoclast survival *in vitro* and *in vivo*. *Am J Pathol* 157:435-448.

Liu L, Igarashi K, Haruyama N, Saeki S, Shinoda H, Mitani H (2004). Effects of local administration of clodronate on orthodontic tooth movement and root resorption in rats. *Eur J Orthod* 26:469-473.

Makkönen N, Hirvonen MR, Teräväinen T, Savolainen K, Mönkkönen J (1996). Different effects of three bisphosphonates on nitric oxide production by RAW 264 macrophage-like cells *in vitro*. *J Pharmacol Exp Ther* 277:1097-1102.

Makkönen N, Salminen A, Rogers MJ, Frith JC, Urtti A, Azhayeva E, *et al.* (1999). Contrasting effects of alendronate and clodronate on RAW 264 macrophages: the role of a bisphosphonate metabolite. *Eur J Pharm Sci* 8:109-118.

Ohta K, Araki N, Shibata M, Hamada J, Komatsumoto S, Shimazu K, *et al.* (1994). A novel *in vivo* assay system for consecutive measurement of brain nitric oxide production combined with the microdialysis technique. *Neurosci Lett* 176:165-168.

Österman T, Kippo K, Lauren L, Hannuniemi R, Sellman R (1995). Effect of clodronate on established collagen-induced arthritis in rats. *Inflamm Res* 44:258-263.

Pennanen N, Lapinjoki S, Urtti A, Mönkkönen J (1995). Effect of liposomal and free bisphosphonates on the IL-1 beta, IL-6 and TNF alpha secretion from RAW 264 cells *in vitro*. *Pharm Res* 12:916-922.

Pilbeam CC, Harrison JR, Raisz LG (2002). Prostaglandins and bone metabolism. In: Principles of bone biology. 2nd ed. Vol. 2. Bilezikian JP, Raisz LG, Rodan GA, editors. San Diego: Academic Press, pp. 979-994.

Plosker GL, Goa KL (1994). Clodronate. A review of its pharmacological properties and therapeutic efficacy in resorptive bone disease. *Drugs* 47:945-982.

Richards PJ, Williams BD, Williams AS (2001). Suppression of chronic streptococcal cell wall-induced arthritis in Lewis rats by liposomal clodronate. *Rheumatology (Oxford)* 40:978-987.

Rogers MJ, Gordon S, Benford HL, Coxon FP, Luckman SP, Mönkkönen J, *et al.* (2000). Cellular and molecular mechanisms of action of bisphosphonates. *Cancer* 88(12 Suppl):2961-2978.

Rygh P (1987). Periodontal response to tooth-moving force: is trauma necessary? In: Orthodontics-state of the art, essence of the science. Graber LW, editor. St. Louis: Mosby, pp. 100-115.

Saito M, Saito S, Ngan PW, Shanfeld J, Davidovitch Z (1991). Interleukin 1 beta and prostaglandin E are involved in the response of periodontal cells to mechanical stress *in vivo* and *in vitro*. *Am J Orthod Dentofacial Orthop* 99:226-240.

Sandy JR, Harris M (1984). Prostaglandins and tooth movement. *Eur J Orthod* 6:175-182.

Shirazi M, Nilforoushan D, Alghasi H, Dehpour A-R (2002). The role of nitric oxide in orthodontic tooth movement in rats. *Angle Orthod* 72:211-215.

Suda T, Takahashi N, Udagawa N, Jimi E, Gillespie MT, Martin TJ (1999). Modulation of osteoclast differentiation and function by the new members of the tumor necrosis factor receptor and ligand families. *Endocr Rev* 20:345-357.

Yamasaki K, Miura F, Suda T (1980). Prostaglandin as a mediator of bone resorption induced by experimental tooth movement in rats. *J Dent Res* 59:1635-1642.

Zhou D, Hughes B, King GJ (1997). Histomorphometric and biochemical study of osteoclasts at orthodontic compression sites in the rat during indomethacin inhibition. *Arch Oral Biol* 42:717-726.

Magnetic motion capture system using *LC* resonant magnetic marker composed of Ni–Zn ferrite core

S. Hashi,[a] M. Toyoda, M. Ohya, and Y. Okazaki
Department of Materials Science and Technology, Gifu University, 1-1 Yanagido, Gifu 501-1193, Japan

S. Yabukami, K. Ishiyama, and K. I. Arai
Research Institute of Electrical Communication, Tohoku University, 2-1-1 Katahira, Aoba-ku, Sendai 980-8577, Japan

(Presented on 1 November 2005; published online 24 April 2006)

We have proposed a magnetic motion capture system using an *LC* resonant magnetic marker. The proposed system is composed of an exciting coil, an *LC* marker, and a 5 × 5-matrix search coil array (25 search coils). The *LC* marker is small and has a minimal circuit with no battery and can be driven wirelessly by the action of electromagnetic induction. It consists of a Ni–Zn ferrite core (3 mmϕ × 10 mm) with a wound coil and a chip capacitor, forming an *LC* series circuit with a resonant frequency of 186 kHz. The relative position accuracy of the system is less than 1 mm within the area of 100 mm^3 up to 150 mm from the search coil array. Compared with dc magnetic systems, the proposed system is applicable for precision motion capture in optically isolated spaces without magnetic shielding because the system is not greatly influenced by earth field noise. © *2006 American Institute of Physics.* [DOI: 10.1063/1.2171927]

I. INTRODUCTION

Effective methods for accurately detecting the motion of unseen objects, such as in an optically shielded space, are strongly required by the medical field for applications such as radiotherapy or endoscopic examinations. In such cases, particularly for measurements within a human body, the applied marker must be small and free from electric wiring. In addition, the location and orientation of the marker must be known exactly during the measurement. Magnetic motion capture systems are believed to satisfy these requirements. There have been several investigations into determining the position of a magnetic object by measuring the magnetic field of the object.[1–6] However, conventional systems require a comparatively large-sized magnetic object as a marker or the marker must contain electric wiring in order to obtain a high signal-to-noise (SN) ratio for the magnetic signal from the marker. To address this, we have proposed and developed a magnetic motion capture system using a magnetically coupled *LC* resonant marker.[7–9] The small-sized marker uses a soft ferrite core with a coil, representing a minimal *LC* circuit with no battery, driven wirelessly by electromagnetic induction. The magnetic signal of the marker is detected by a matrix-designed search coil array. Our proposed system allows the approximate orientation of the marker and the position of the marker to be determined accurate to within 1 mm under limited conditions.[9] In this paper, we examine the accuracy of the proposed system in detecting the position and orientation of the marker over a wide area in order to expand the detectable space.

II. SYSTEM COMPONENTS AND THEORY

Figure 1 shows a schematic diagram of the motion capture system. The system is composed of the measurement equipment and a coil assembly, consisting of a driving coil, an *LC* marker, and a pickup coil array. As shown in the figure, we use the right-handed coordinate system. Figure 2 shows a photograph of the coil system and the *LC* marker. The marker consists of a Ni–Zn ferrite core (3 mm in diameter and 10 mm long) with 335 turns of wound coil and a chip capacitor (680 pF), representing an *LC* series circuit designed for a resonant frequency of 186 kHz. The search coil array consists of 25 coils placed at intervals of 45 mm on an acryl board, configuring a matrix layout. Each coil is made of 100 turns of polyester enameled copper wire (PEW) around an acryl bobbin of 25 mm in diameter. A sinusoidal excitation of 22 V was applied to the driving coil (ten turns of PEW around an acryl coil 210-mm square) and the marker was strongly excited at its resonant frequency by electromagnetic induction. In this paper, the square-shaped driving coil is adopted to improve the SN ratio for pickup coils placed around the four corners. As a result, the SN ratio increased up to 15% for these coils.

The induction field of the marker is used to determine the position and orientation of the marker. However, the induced voltage detected at the pickup coils includes both the induction of the exciting field and the marker field, as they

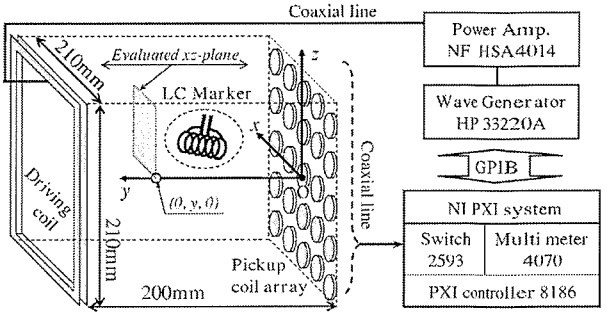

FIG. 1. Schematic diagram for the proposed motion capture system.

[a]Electronic mail: nashi@cc.gifu-u.ac.jp

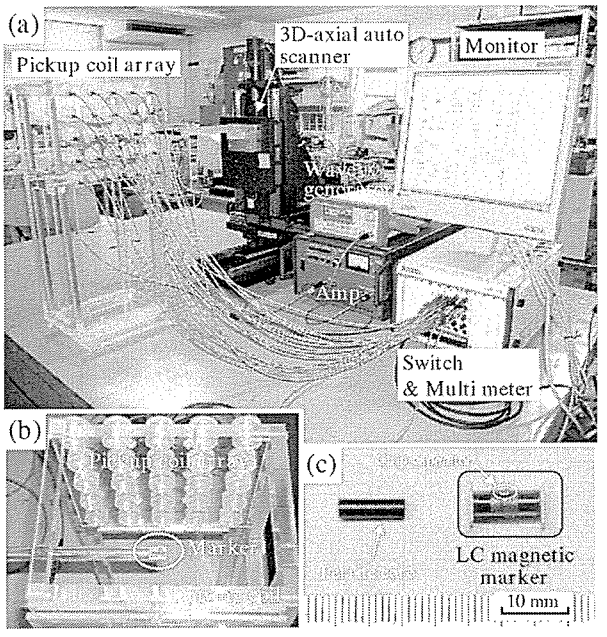

FIG. 2. Pictures of (a) developed motion capture system, (b) detecting part of the motion system, and (c) *LC* resonant magnetic marker with high permeability Ni–Zn ferrite core.

have the same frequency. To extract the marker contribution, the induced voltage is first measured without the marker and then measured with the marker. The marker voltage is then obtained by subtracting as vectors the induced voltage without the marker from the induced voltage with the marker.[7–9] The position and orientation of the marker is calculated using the following equations [Eqs. (1), (2), and (3)], which effect an optimization using the Gauss-Newton method:[10]

$$S(\boldsymbol{p}) = \sum_{i=1}^{n} (\boldsymbol{B}_{\mathrm{meas}}^{(i)} - \boldsymbol{B}_{\mathrm{cal}}^{(i)}(\boldsymbol{p}))^2 \rightarrow \text{Minimum}, \tag{1}$$

$$\boldsymbol{B}_{\mathrm{cal}}^{(i)}(\boldsymbol{p}) = \frac{1}{4\pi\mu_0}\left\{-\frac{\boldsymbol{M}}{r_i^3} + \frac{3(\boldsymbol{M}\cdot\boldsymbol{r}_i)\cdot\boldsymbol{r}_i}{r_i^5}\right\}, \tag{2}$$

$$\boldsymbol{p} = (x, y, z, \theta, \phi, M). \tag{3}$$

Here $S(\boldsymbol{p})$ is an objective function (the least squares value), i is the coil number, n is the total number of coils, $\boldsymbol{B}_{\mathrm{meas}}^{(i)}$ is the measured flux density, $\boldsymbol{B}_{\mathrm{cal}}^{(i)}$ is the theoretical flux density that takes into account the magnetic dipole field, $\boldsymbol{p}$ is the parameters of the marker, $\boldsymbol{M}$ is the magnetic moment, (x, y, z) is the position of the marker, $\boldsymbol{r}$ is the equation of an ideal dipole field expressed as a function of position and orientation, θ is the angle between the x axis and the direction vector when the moment is projected on an xy plane, and ϕ is the angle between the direction of the moment and the z axis.

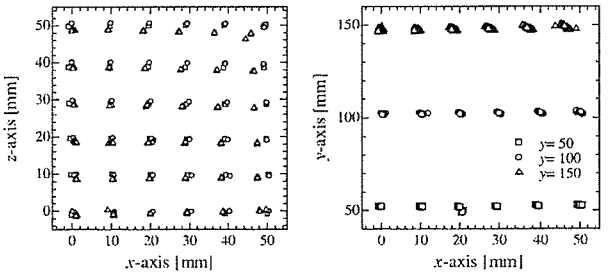

FIG. 3. Evaluation results for the developed motion capture system (xy-plane and xz-plane plot).

III. RESULTS AND DISCUSSION

Figures 3(a) and 3(b) show the measured position of the marker orientated parallel to the y axis as it was swept in 10-mm steps along a grid pattern in the xz plane at $y=50$, 100, and 150 mm, measured by a precision three-dimensional-axial auto scanner [the marker was put on the end of a rod made of nonmagnetic resin, as shown in Fig. 2(b)]. Each point represents ten measurements at every marker position, with triangles for $y=50$ mm, circles for $y=100$ mm, and squares for $y=150$ mm. Good accuracy is seen in the position of the marker at $y=50$ mm and $y=100$ mm.

To capture the exact motion of the marker, the angle of the orientation of the marker must be measured. Figures 4(a) and 4(b) show the measured angles θ and ϕ, respectively. The figures show that approximately correct angles, $\theta=\phi=90°$, were acquired at $y=50$ mm and $y=100$ mm. However, at $y=150$ mm, a wide dispersion of θ and ϕ was measured, particularly when the marker was located far from the center of the system. This was due to the fact that the marker was not excited efficiently at these positions, degrading the SN ratio, because the deviation angle between the exciting field vector and the normal vector of the marker approached a right angle.

The relative error of the measured position of all the points at each y value was evaluated and expressed as an averaged value with a standard deviation. The results are as follows: 0.14 ± 0.60 mm at $y=50$ mm, 0.14 ± 0.19 mm at $y=100$ mm, and -0.60 ± 0.37 mm at $y=150$ mm. According to the results, the relative position accuracy was less than 1 mm.

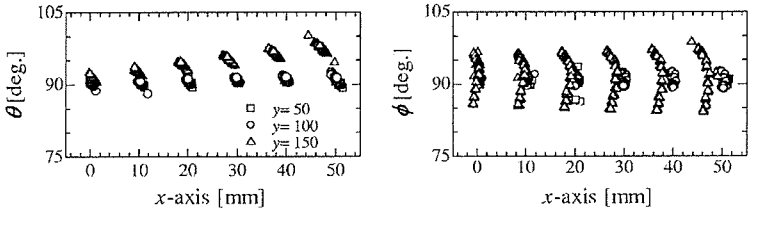

FIG. 4. Evaluation results for attitude angles (a) θ and (b) ϕ.

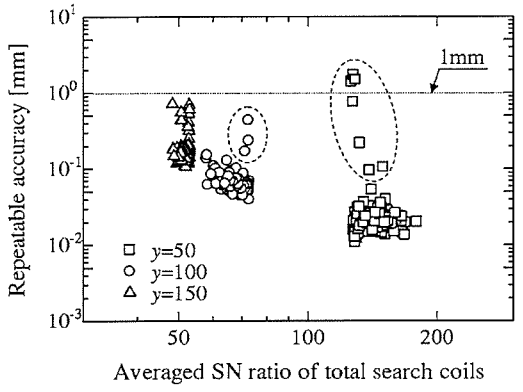

FIG. 5. The averaged SN ratio dependence of the repeatable position accuracy.

Figure 5 shows the relation between the averaged SN ratio of the total search coils and the repeatable position accuracy. The noise level of the system was estimated to be 3 μV. It can be seen that the repeatable accuracy improved as the averaged SN ratio increased. However, several points of poor repeatable accuracy at a high SN ratio are seen at $y=50$ and 100 mm. It is thought that these points indicate the presence of coordinates with a local minimum due to the regular arrangement of the search coil array. It is believed that an asymmetrical arrangement of the search coils would eliminate such coordinates with local minima.

Overall, the results show that the system is capable of capturing the motion of the marker wirelessly with a high accuracy in the millimeter scale.

IV. CONCLUSION

The performance of a proposed magnetic motion capture system using an *LC* resonant magnetic marker was evaluated. The relative position accuracy was found to be less than 1 mm and improved as the average SN ratio increased. The approximate orientation of the marker could be determined when the marker was located within the area of 100 mm^3 up to 150 mm from the pickup coil array, except in the region where the deviation angle between the direction of the exciting field at the marker and the normal vector of the marker was nearly equal to 90°.

ACKNOWLEDGMENTS

This study was supported by the Industrial Technology Research Grant Program 03A47063a of the New Energy and Industrial Technology Development Organization (NEDO) of Japan. This study was also supported by Strategic Information and Communications R&D Promotion Programme (SCOPE) in the Ministry of Public Management, Home Affairs, Posts and Telecommunications (MPHPT).

[1]F. Grant and G. West, *Interpretation Theory in Applied Geophysics* (McGraw-Hill, New York, 1965).
[2]S. V. Marshall, IEEE Trans. Veh. Technol. **VT-27**, 65 (1978).
[3]W. M. Wynn, C. P. Frahm, P. J. Carroll, R. H. Clark, J. Wellhoner, and M. J. Wynn, IEEE Trans. Magn. **MAG-11**, 701 (1975).
[4]J. E. Mcfee and Y. Das, IEEE Trans. Antennas Propag. **AP-29**, 282 (1981).
[5]S. Yabukami, K. Arai, H. kanetaka, S. Tsuji, and K. I. Arai, J. Magn. Soc. Jpn. **28**, 711 (2004).
[6]J. A. Paradiso, K. Hsiao, J. Stricken, J. Lifton, and A. Adler, IBM Syst. J. **39**, 892 (2000).
[7]S. Yabukami, S. Hashi, Y. Tokunaga, T. Kohno, K. I. Arai, and Y. Okazaki, J. Magn. Soc. Jpn. **28**, 877 (2004).
[8]S. Hashi, Y. Tokunaga, S. Yabukami, T. Kohno, T. Ozawa, Y. Okazaki, and K. I. Arai, J. Magn. Magn. Mater. **290–291**, 1330 (2005).
[9]Y. Tokunaga, S. Hashi, S. Yabukami, T. Kohno, M. Toyoda, T. Ozawa, Y. Okazaki, and K. I. Arai, J. Magn. Soc. Jpn. **29**, 153 (2005).
[10]T. Nakagawa and Y. Koyanagi, *Experimental Data Analysis by the Least Square Method* (The University of Tokyo Press, Tokyo, 1982).

J. Magn. Soc. Jpn., 30, 391–395 (2006)

〈Paper〉

Development of Wireless Magnetic Multi-position Detecting System Using FFT Analysis

M. Toyoda, S. Hashi, S. Yabukami*, M. Ohya, K. Ishiyama*, Y. Okazaki, K. I. Arai*

Faculty of Engineering Gifu University, *1-1 Yanaido, Gifu 501-1193, Japan*

*Research Institute of Electrical Communication, Tohoku University, *2-1-1 Katahira, Aoba-ku, Sendai 980-8577, Japan*

A wireless multi-position detecting system using three *LC* resonant magnetic markers was developed and demonstrated. The markers were given individual resonant frequencies of 183 kHz, 487 kHz, and 730 kHz, respectively. The new measuring technique described in this paper was applied to the system in order to reduce the acquisition time: the markers were excited by a superposed wave corresponding to the resonant frequencies, while the voltage signals induced through the pickup coils are separated into each frequency spectrum by *FFT* analysis. Regardless of the number of markers, the necessary voltage amplitude of each frequency spectrum can be obtained easily at the same time. Thus, our proposed system can detect multiple markers at a time. All the positional accuracies of the three markers are less than 5 mm within 100 mm of the pickup coil array.

Key words: multi-position detecting, *LC* resonant magnetic marker, wireless sensing, *FFT* analysis

複数LC共振型磁気マーカを用いた多点位置検出システム

豊田征治，柾修一郎，薮上信*，大矢雅志，石山和志*，岡崎靖雄，荒井賢一*

岐阜大学工学部，岐阜市柳戸 1-1（〒501-1193）

*東北大学電気通信研究所，仙台市青葉区片平 2-1-1（〒980-8577）

1. はじめに

これまでにモーションキャプチャに代表される3次元空間内における物体の位置や方向を計測する手法については，様々な方式が考案され実用化されている[1)-5)]．しかしながら検出対象物が光学的に遮蔽された空間に存在し，貼付するマーカへの配線が困難または望ましくないような状況下で高精度な計測を行う方式はほとんど見あたらない．そこで著者らは，このような状況に対応可能な，*LC*共振型ワイヤレス磁気マーカ（以下，*LC*マーカと呼ぶ）を用いた位置・方向検出手法を提案し検討を行っている．この方式で用いるマーカは配線およびバッテリの搭載が不要なため小型化が可能であり，また *LC* マーカに異なる共振周波数を個別に設定することで多点計測が可能となるため，例えば，指先など生体の複雑な動きを正確に捉える用途に適している．具体的な応用例として仮想空間内における入力デバイスが挙げられる．これは，指先に添付したマーカの位置を検出し各指先の動きをトレースすることで，仮想的なキーボード操作を可能にするものである．この例では，指の動きによってマーカがセンサの死角に入る場合が考えられる．また指の自然な動作を妨げないように，マーカは小型・軽量で駆動のための配線が無いことが望ましいと言える．Table 1 は本論文で試作したシステムと他のシステムとの仕様を比較できるようまとめたものである．本システムに比べて他のシステムでは以下のような問題点が挙げられる．同じ交流磁気式ではマーカに配線が必要であること，永久磁石を用いた直流磁気式ではマーカ数が 2 個までに限られ，また地磁気の影響を受け易いこと，光学式についてはマーカがカメラの死角に入った場合や背景に対してマーカのコントラストが十分得られない場合には検出不可能になること，多点計測の際に全てのマーカの動きを視認できる位置にビデオカメラを配置する必要があるため設置位置の自由度が少ないことが挙げられる．しかし，*LC*マーカを用いたシステムではこれらの問題を解決可能であると考えられる．我々はこれまでに，この手法を用いたシステムを試作し，100 mm 立方の空間内に配置した 1 個の *LC* マーカの位置および方向を，計測速度 1 Hz 程度，相対位置精度 2 mm 以下で検出可能であることを示してきた[6)-8)]．

Table 1 Specification comparison of proposed system with other system.

	This paper	AC magnetic	DC magnetic[11)]	Optical
System	LC resonant magnetic marker / Pickup coil	AC magnetic field source 3-axial magnetic sensor	Permanent magnet Hole sensor	Luminescent, Color contrast Video camera
Wired/Wireless	Wireless	Wired	Wireless	Wireless
Detectable range	50-100 mm	≦ 760 mm	≦ 50 mm	≦ 30 m
Position acuracy	5 mm cubic	0.76 mm cubic	0.3 mm cubic	range / 1,000
Detection speed	1 Hz (3 Hz)*1	120 Hz	100 Hz	60 Hz
Number of markers	≧ 3*2	≦ 16	≦ 2	≦ 64

*1 Under a sufficient number of instruments and CPUs, *2 Under consideration.

今回，著者らはこのシステムを更に発展させ，複数個の *LC* マーカの位置および方向を同時に検出するシステムを試作し，多点計測に関する基礎検討を行った．本論文に示すシステムの特徴は，個々の *LC* マーカに異なる共振周波数を設定することによって各マーカを同時かつ個別に検出できる点である．このために，*LC* マーカに印加する励磁磁界に複数の周波数成分を重畳した重畳励磁波を用いた．また，磁界検出コイルの誘起電圧の測定には高速サンプリングが可能なデジタイザを用いて誘起電圧波形を取得し，得られた波形データを *FFT* 解析することにより個別の周波数成分に分離して電圧振幅を得る方式を採用するなど，計測系の見直しを行った．更に，過去に報告されている永久磁石をマーカに用いた直流磁気式[9]に対する優位性を示すため，3 個の *LC* マーカを用いた同時検出についての検討を行った．その結果，Table 1 に示すように，検出コイルアレイから 50～100 mm の範囲を 5 mm 立方以内のばらつきで 3 個のマーカを同時検出可能であることが明らかとなった．以下にその詳細を報告する．

2. システムの構成と位置検出原理

2.1 システムの構成

構築したシステムの模式図を Fig. 1 に示す．直径 210 mm のテフロン製ボビンに巻かれた励磁コイル（線径 0.26 mm×10 回巻き）と，直径 25 mm のアクリル製ボビンに巻かれた 25 個の検出コイル（線径 0.1 mm×50 回巻き）が 45 mm 間隔で 5×5 のマトリクス状に配置されている検出コイルアレイを 150 mm の間隔且つ励磁コイルおよび検出コイルアレイ中心に配置した検出コイルの中心軸が一致するように対置している．また，各検出コイルはスイッチモジュールを介して誘起された電圧波形を計測するためのデジタイザに接続されている．これに加えて，励磁波を生成するための任意波形発生装置およびパワーアンプと，システム全体を制御し *LC* マーカの位置を算出するためのパソコンから成る．今回使用したデジタイザは 2 系統の入力端子を有しているため，スイッチモジュールを 2 台用いて，それぞれに 13 個と 12 個の検出コイルを割り当て，同時に 2 個ずつの検出コイルの電圧測定を行うことが可能である．

外部磁界による駆動が可能な *LC* 共振型磁気マーカを Fig. 2 に示す．直径 3 mm，長さ 10 mm のフェライト磁心（TDK 製 PC40，Mn-Zn フェライト，$\mu_i = 2{,}300$，$B_s = 0.51$ T）に施した 335 回の巻線の両端にチップコンデンサが接続されている．これよりマーカ自身が *LC* 共振回路を構成している．また今回作製した *LC* マーカ 3 個の仕様を Table 2 に示す．各マーカはコイル巻数とコンデンサ容量によって共振周波数を変化させているが，サイズは全て Fig. 2 に示すように，直径 4 mm，長さ 10 mm，重さは 0.64g 程度である．また *LC* マーカは，Fig. 1 に示すような座標系を設定し，非磁性，非金属の台座によって検出空間内に，1 mm 程度の設置精度で配置した．

2.2 誘起電圧計測方法

検出空間内に配置された *LC* マーカの位置と方向を求めるには，*LC* マーカから発生される誘導磁界を検出コイルによって測定する必要がある．しかし，*LC* マーカを駆動するための励磁磁界と *LC* マーカの発する誘導磁界は同じ周波数成分を持つため，直接測定することは困難である．しかし，以下の手順を経ることで間接的に測定することが可能である．

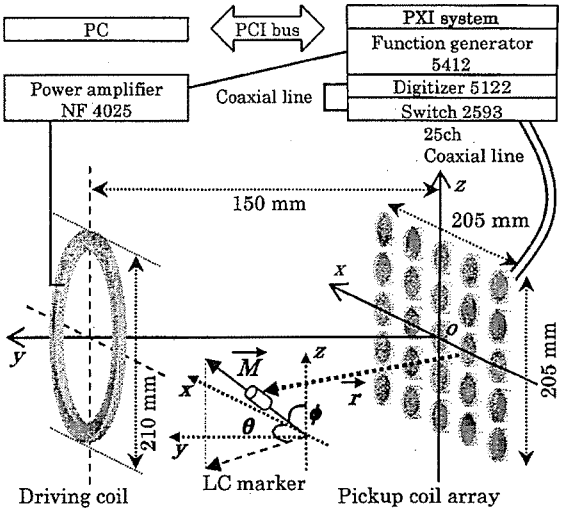

Fig. 1 Schematic diagram of the system.

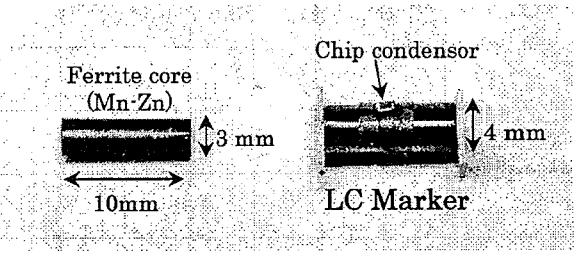

Fig. 2 Shape of the LC resonant magnetic marker.

検出コイルに誘起される電圧について，検出空間内の *LC* マーカの有無に対する *LC* マーカ共振周波数付近の周波数特性を Fig. 3 (a)に示す．また両者の差分をとった結果を Fig. 3 (b)に示す．これらが共振周波数の前後に極値を持つのは，励磁磁界に対して誘導磁界の位相が大きくずれるためである．このピーク－ピーク電圧が *LC* マーカの発する磁界強度に比例することから，本論文ではマーカ寄与電圧 V_{MK} と定義し，検出コイル毎の V_{MK} を用いて，2.3 で述べる算出原理に基づいて位置および方向を求めている．しかし，Fig. 3 (b)に示すようにマーカ 1 個につき 2 点の周波数（f_1, f_2）の電圧計測を行う必要があり，電圧計測器として DMM (Digital Multi-Meter) を用いた以前のシステムでは[7]，マーカ個数の増加に伴って測定周波数を切り替える回数が増加し，計測速度の低下が懸念される．Fig. 4 は，3 個の *LC* マーカの V_{MK} を測定する場合の周波数特性の概略図である．3 個の場合，各 *LC* マーカの共振周波数前後の f_1 ～ f_6 についての電圧を計測し V_{MK} を得る必要がある．

そこで，必要な複数の周波数成分を重畳させた重畳波（PC 上で作成）でマーカの励磁を行い，高速サンプリングが可能なデジタイザで誘起電圧波形を測定し，PC 上で *FFT* 解析を行うことで各周波数成分のスペクトル強度として電圧振幅を得る手法を用いた．これにより *LC* マーカの数に依存せず同時に複数の周波数成分の電圧測定が可能となる．Fig. 3 (a)にその概念図を示す．また，*FFT*

Table 2 Specifications of LC markers.

	Marker 1	Marker 2	Marker 3
Resonant frequency (kHz)	183	487	730
f_1 (kHz)	182	481	720
f_2 (kHz)	185	492	740
Diameter of core (mm)	3	3	3
Coil turns	335	335	280
Condensor (pF)	680	68	33
Inductance (μH)	1026	1598	1546
Quality factor	59	27	27

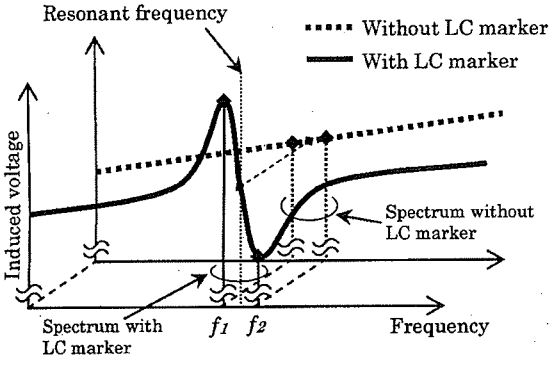

(a) Influence on the induced voltage of the LC marker, and amplitude spectrum after FFT

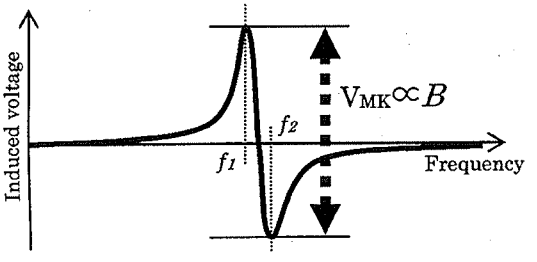

(b) Marker's contribution voltage

Fig. 3 Background and marker's contribution.

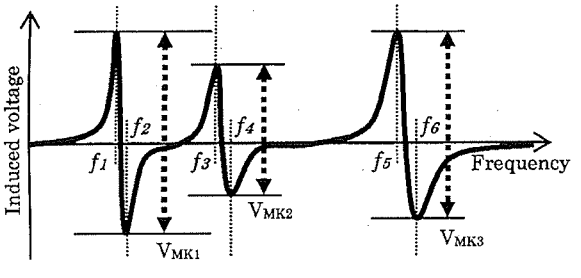

Fig. 4 Marker's contribution voltage when three markers are detected.

解析後のスペクトルの周波数分解能はデジタイザのサンプリング周波数とサンプリング数に依存するが，サンプリング数が増えると *FFT* 解析にかかる時間が増加する．一方，本論文のシステムではスイッチの切り替えおよびその安定までの待機時間が必要なため，*FFT* の計算にかかる時間はスイッチが安定するまで十分待機

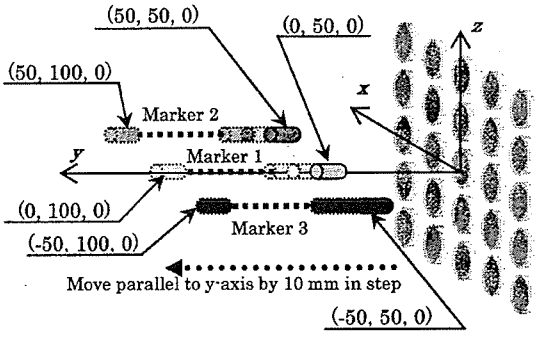

Fig. 5 Arrangement of the markers and pick-up coil array.

できる時間と同程度になるよう検討した結果，サンプリング数を 50, 000 個とした．これに対し *FFT* 解析の周波数分解能が 1 kHz になるように，サンプリング周波数を 50 MHz とした．

2.3 位置算出原理

本研究では *LC* マーカから発生する誘導磁界をダイポール磁界に近似できると仮定して，式(1)〜(3)からマーカの位置および方向を算出し，Gauss-Newton 法[10] により最適化を行った．

$$S(\vec{p}) = \sum_{i=1}^{n} \left| \vec{B}^{(i)}_{meas} - \vec{B}^{(i)}_{cal}(\vec{p}) \right|^2 \rightarrow Minimum \qquad (1)$$

$$\vec{B}^{(i)}_{cal}(\vec{p}) = \frac{1}{4\pi} \left\{ -\frac{\vec{M}}{r_i^3} + \frac{3(\vec{M} \cdot \vec{r}_i) \cdot \vec{r}_i}{r_i^5} \right\} \qquad (2)$$

$$\vec{p} = (x, y, z, \theta, \phi, M) \qquad (3)$$

ここで $S(\vec{p})$ は評価関数，n は検出コイルの数，i は検出コイルの番号(1〜25)，$\vec{B}^{(i)}_{meas}$ は検出コイル i における磁束密度の測定値，$\vec{B}^{(i)}_{cal}$ はダイポール磁界を考慮した検出コイル i における磁束密度の理論値，$\vec{r}_i$ は検出コイル i の中心からマーカまでの位置ベクトル，$\vec{M}$ はマーカの磁気モーメント，θ は xy 平面に射影したモーメントの方向ベクトルと x 軸とのなす角，ϕ はモーメントの方向ベクトルと z 軸のなす角(Fig. 1 参照)，$\vec{p}$ はマーカのパラメータにより構成されるベクトル量である．

3. 実験結果および考察

3 個の *LC* マーカ(1〜3)を Fig. 5 のように x 軸と平行な直線上に並べ，10 mm 刻みで $50 \leqq y \leqq 100$ の範囲の各位置において 100 回ずつマーカの位置・方向の検出を行った．各 *LC* マーカはマーカのコイル部の中心軸と励磁コイルおよび検出コイルの中心軸が平行（$\theta = 90°$，$\phi = 90°$）になるように設置した．なお，*LC* マーカの実際の設置座標は検出コイル側のマーカ端面の中心を基準とした．

Fig. 6 は，検出の結果を (a) xy 平面，(b) yz 平面から見たものである．各検出位置における *LC* マーカの信号対雑音比(S/N 比) を数値で示した．なお，この S/N 比は各検出コイル 25 個の S/N 比の二乗和平均値で算出しており，本システムのノイズレベルは 30 μV 程度であった．Fig. 6 より，どの位置でも検出位置のばらつきはおよそ 5 mm 立方以内となった．標準偏差で評価した検出位置のばらつきと S/N 比の関係を Fig. 7 に示す．図から，S/N 比が低

い位置ではばらつきが大きくなることが分かる．S/N 比が1桁台にもかかわらず検出位置のばらつきがこの程度に収まっているのは，マーカとの距離が比較的近い検出コイルの S/N 比は高いが，全体としては S/N 比が低いものが多いためである．

また Fig. 6 (a)より，検出コイルからの距離が大きくなるにしたがって，マーカ 2 およびマーカ 3 の検出位置が徐々に中心へすぼんでいくことが分かる．実際の *LC* マーカの設置位置には 1 mm 程度の不確定さがあるが，このずれはそれを超えているため，S/N 比の低い検出コイルの配置に原因があるのではないかと考えた．そこで，マーカ 2 を座標 (50, 100, 0)に配置したときの実測データから S/N 比がそれぞれ 3 および 5 以下となる検出コイルの配置を調べ，各検出コイルのデータを式(2)より求められるダイポール磁界がつくる理論値に置き換えて位置算出を行い，実測値のみの場合と比較した結果を Fig. 8 に示す．これより S/N 比の低い検出コイルのデータを理論値に置き換えることで，算出位置が実際のマーカ設置位置に近づくことがわかる．また Fig. 9 に，マーカ 2 の設置位置がそれぞれ(a) (50, 50, 0)，(b) (50, 100, 0)のときの各検出コイルの S/N 比の分布を示した．Fig. 9 (a) に示すように，マーカが検出コイルアレイに対して比較的近い位置にある場合はマーカに近い検出コイルの S/N 比が高いため，S/N 比の低い検出コイルの影響を受けにくいが，Fig. 9 (b)では S/N 比が最大のものでも 30 程度しかなく，更に S/N 比の低い検出コイルがマーカから見て右よりに偏っていることがわかる．以上のことから，S/N 比が全体的に低く，また S/N 比が 5 以下の検出コイルがアレイの片側に偏って存在するような場合にはマーカの検出位置への影響が大きくなるものと思われる．なお，Fig. 9 に示す S/N 比について，検出コイルアレイに対する *LC* マーカの配置や姿勢角によって，マーカの発する磁界ベクトルの検出コイルへの鎖交状況は大きく変化するため，単純にマーカと検出コイルの距離に対応した値にはならず，ある一定の距離を境に検出コイル裏側から回りこんで鎖交する磁界ベクトルの影響も考慮する必要がある．

また，検出にかかった時間を Fig. 10 に示す．検出コイル 25 個

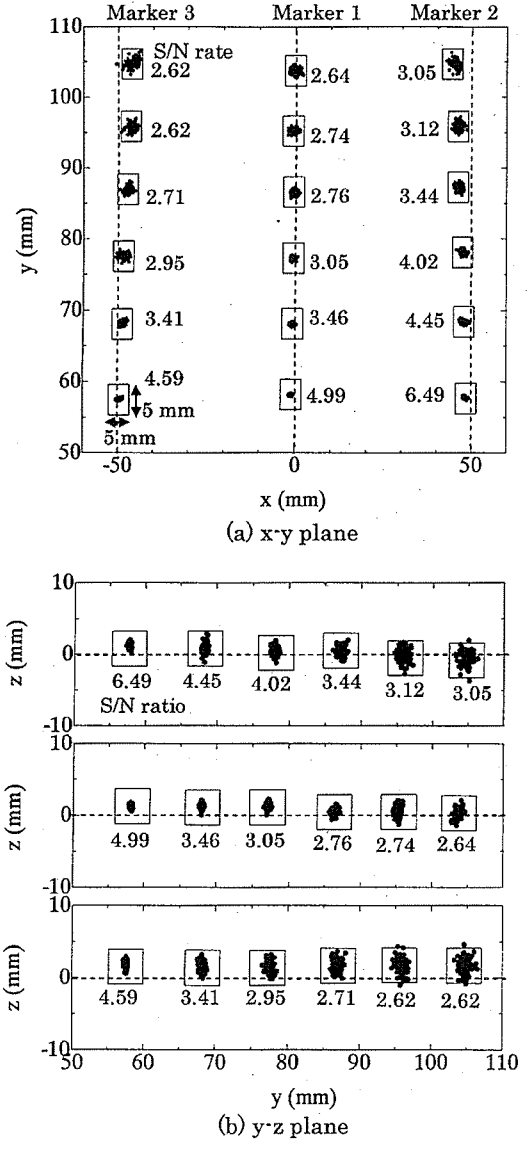

Fig. 6 Calculated position and S/N ratio of each position.

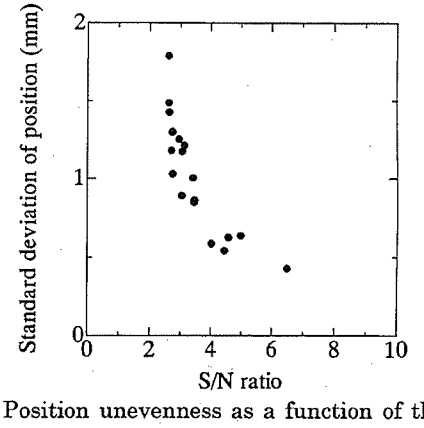

Fig. 7 Position unevenness as a function of the S/N ratio.

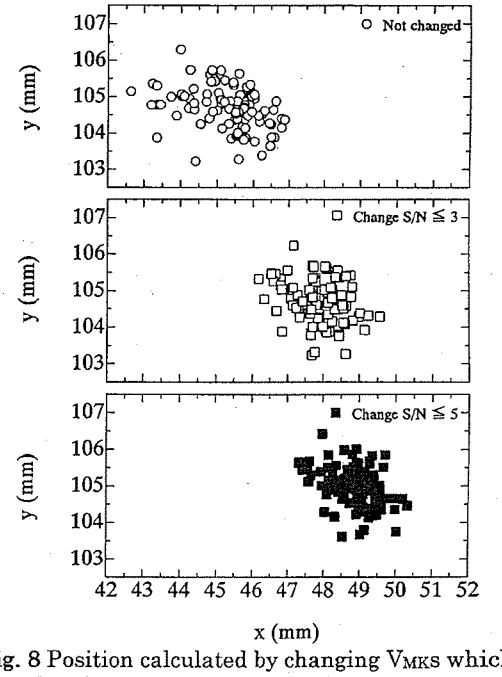

Fig. 8 Position calculated by changing V_{MKS} which have low S/N ratios to theoretical values.

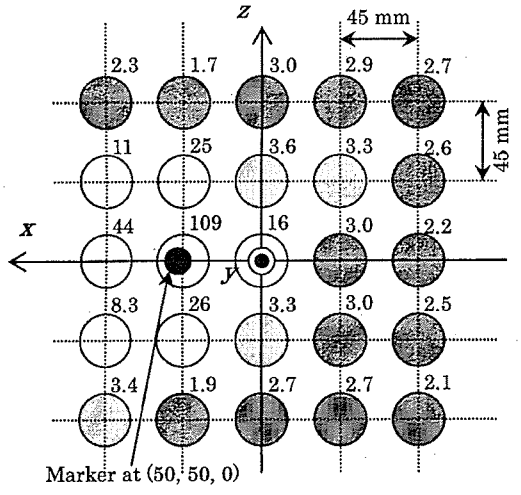

(a) Marker at (50, 50, 0)

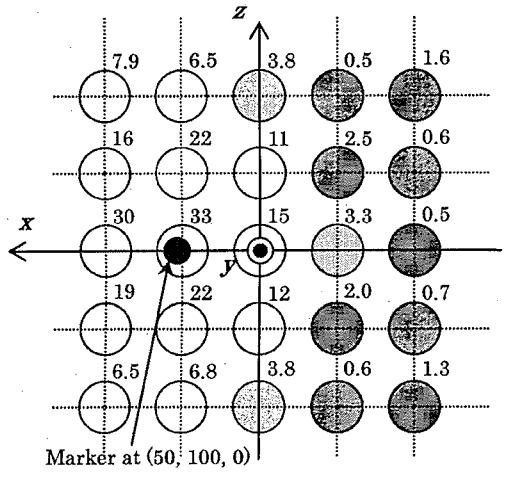

(b) Marker at (50, 100, 0)

Fig. 9 S/N ratio of each pickup coil (S/N ratio of light grey coils ≦ 5, dark grey coils ≦ 3).

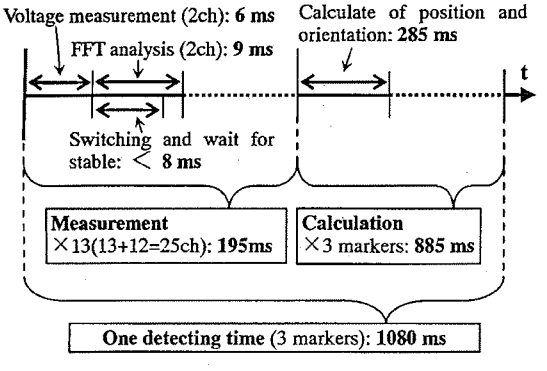

Fig. 10 An acquisition time chart for the motion of the marker.

分の電圧計測および*FFT*変換に195 ms，位置算出に3個で885 ms (1個のマーカあたり295 ms)，1回の検出あたりで1080 ms，検出速度としておよそ1 Hzという結果を得た．ただし，計測器を各検出コイル分，また算出用CPUを各*LC*マーカ分用意することで，検出にかかる時間は1 chの電圧測定にかかる15 msとマーカ1個にかかる295 msの和の310 msとなり，検出速度にして3 Hz程度が実現可能である．位置算出アルゴリズムの最適化によって更なる高速化が可能であると考えられる．また一度に検出可能なマーカの数については，現時点では詳細な検討を行っておらず今後の課題であるが，マーカ共振回路の性能指数や検出コイルの周波数特性について検討を行うことで更に増やすことが可能である．

4. まとめ

重畳励磁波とデジタイザを用いた*FFT*解析による複数個の*LC*マーカの位置検出手法を提案し検討を行った．以下に得られた知見を示す．

（1）3個の*LC*マーカの位置検出を行った結果，検出コイルアレイから50～100 mmの範囲で検出位置は5 mm立方程度のばらつきであった．

（2）3個の*LC*マーカの位置を検出するのに要する時間は1080 msで測定速度にするとおよそ1 Hzであった．その内訳は電圧計測に195 ms，3個の*LC*マーカの位置算出に885 msであった．

（3）*LC*マーカをある特定の領域に配置したとき，S/N比が低い検出コイルが検出コイルアレイ中に偏って分布し，実際のマーカの位置よりも数mm程度ずれて検出されることがわかった．

謝辞 本研究の一部は新エネルギー・産業技術総合開発機構の「産業技術研究助成事業」(プロジェクトID:03A47063a)により行った．また本研究の一部は総務省の「戦略的情報通信研究開発制度」(5E5番126号)の助成により行った．

References

1) F. R. Raab, E. B. Blood, T. O. Steiner, and H. Jones, *IEEE Trans. Aero. Electro.*, **AES-15**, 709 (1979).
2) S.V. Marshall, *IEEE Trans. Vehicular Technology*, **VT-27**, 65 (1978).
3) W.M. Wynn, C.P. Frahm, P.J. Carroll, R.H. Clark, J. Wellhoner, M.J. Wynn, *IEEE Trans. Magn.*, **MAG-11**, 701 (1975).
4) J. E. Mcfee, Y. Das, *IEEE Trans. Antennas and propagation*, **AP-29** 282 (1981).
5) N. M. Prakash and F. A. Spelman, *Proc. 19th Inter. Conf. IEEE/EMBS*, 2394 (1997).
6) S. Yabukami, S. Hashi, Y. Tokunaga, T. Kohno, K. I. Arai, and Y. Okazaki, *J. Magn. Soc. Jpn.*, **28**, 877 (2004).
7) Y. Tokunaga, S. Hashi, S. Yabukami, T. Kohno, M. Toyoda, T. Ozawa, Y. Okazaki and K. I. Arai, *J. Magn. Soc. Jpn.*, **29** 153 (2005).
8) S. Hashi, Y. Tokunaga, S. Yabukami, T. Kohno, T. Ozawa, Y. Okazaki, K. Ishiyama and K. I. Arai, *J. Magn. Magn. Mater*, **290-291**, 1330 (2005).
9) S. Yabukami, H. Kikuchi, M. Yamaguchi, K.I. Arai, A. Itagaki and N. Wako, *IEEE Trans. Magn.*, **36**, 3646 (2000).
10) T. Nakagawa, Y. Koyanagi, Experimental Data Analysis by the least square method, (in Japanese) p. 95, (The University of Tokyo Press, Tokyo, 1982).
11) S. Yabukami, K. Arai, H. Knetaka, S. Tsuji, K.I. Arai, *J. Magn. Soc. Jpn.*, **28**, 711 (2004).

2005年10月19日受理，2006年2月21日採録

Wireless Magnetic Motion Capture System for Multi-Marker Detection

Shuichiro Hashi[1], Masaharu Toyoda[1], Shin Yabukami[2], Kazushi Ishiyama[2], Yasuo Okazaki[1], and Ken Ichi Arai[2]

[1]Department of Materials Science and Technology, Gifu University, 1-1 Yanagido, Gifu 501-1193, Japan
[2]Research Institute of Electrical Communication, Tohoku University, 2-1-1 Katahira, Sendai 980-8577, Japan

A wireless multi-motion capture system using five LC resonant magnetic markers has been developed and is demonstrated. Each marker has an individual resonant frequency, 157, 201, 273, 323, and 440 kHz, respectively. A new measuring technique is applied in order to reduce the acquisition time. In this new technique the markers are excited by a superposed wave corresponding to the all resonant frequencies, while the voltage signals induced through pick-up coils are separated in a frequency spectrum by FFT analysis. Regardless of the number of markers, the voltage amplitude for each resonant frequency can be easily obtained simultaneously and thus the proposed system can detect multiple markers. The positional accuracy for five markers is less than 2 mm within 100 mm of the pick-up coil array.

Index Terms—**FFT analysis, LC resonant magnetic marker, multi-marker, wireless motion capture system.**

I. Introduction

WIRELESS motion capture for multi-point detection at close range is a candidate technique for virtual input devices or medical treatment applications. In such applications, particularly for measurements of the motion of fingers, the markers used must be small and free from electric wiring to allow normal motion. In addition, the location and orientation of the markers must be known exactly during the measurement. Furthermore, if a dead angle is likely to occur, an optical method is unfavorable. There have been several investigations into determining the position of a magnetic object by measuring its magnetic field [1]–[6]. However, conventional systems require a comparatively large magnetic object as a marker or the marker must contain electric wiring, in order to obtain a high SN ratio for the magnetic signal from the marker. To address this, we have proposed and developed a wireless magnetic motion capture system using a magnetically-coupled LC resonant marker [7], [8]. The small sized marker uses a soft ferrite core with a coil, representing a minimal LC circuit with no battery, driven wirelessly by electromagnetic induction. The magnetic signal of the marker is detected by a matrix-designed pick-up coil array. Our proposed system allows the approximate orientation and the position of a single marker to be determined accurate to within 1 mm in a space 150 mm from the pick-up coil array. It also allows multi-point detection because the system allows the use of several markers with individual frequencies. In this paper, we extend our system to detect multiple markers and we examine the accuracy of the system in detecting the positions and orientations of the markers.

II. Components and Measuring Method of the System

Fig. 1 shows a schematic diagram of the motion capture system for multi-marker detection. The system is composed of measurement instruments and a coil assembly, consisting of a driving coil, LC markers, and a pick-up coil array. The marker consists of a Ni-Zn ferrite core (3 mm in diameter and 10-mm long) with a wound coil and a chip capacitor, representing an LC series circuit designed for resonant frequencies of 157, 201, 273, 323, and 440 kHz. The pick-up coil array consists of 25 coils placed at intervals of 45 mm on an acryl board, configuring a matrix layout. Each coil is made of 40 turns of polyester enameled copper wire (PEW) around an acryl bobbin 25 mm in diameter. An excitation of 22 V is applied to the driving coil (10 turns of PEW around the Teflon coil, 200 mm in diameter) and the markers are strongly excited at their resonant frequency by electromagnetic induction. However, the system becomes slow with an increase in the number of markers, owing to time required to switch frequencies and make multiple measurements. In this paper, a new signal measurement method is adopted to increase the system speed. All the markers are excited simultaneously by a superposed wave corresponding to all the resonant frequencies of the markers. As shown in Fig. 2, the induced wave measured by the pick-up coil is analyzed into a frequency spectrum by FFT analysis. First, the spectrum is measured without the markers and then the spectrum is

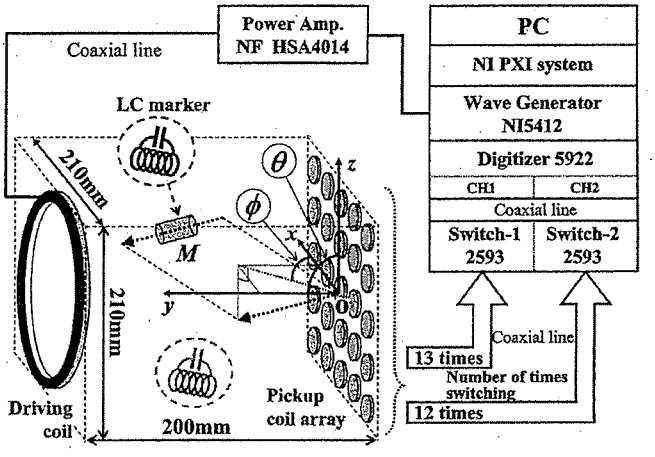

Fig. 1. Schematic diagram of the proposed wireless motion capture system for multiple markers.

Digital Object Identifier 10.1109/TMAG.2006.880737

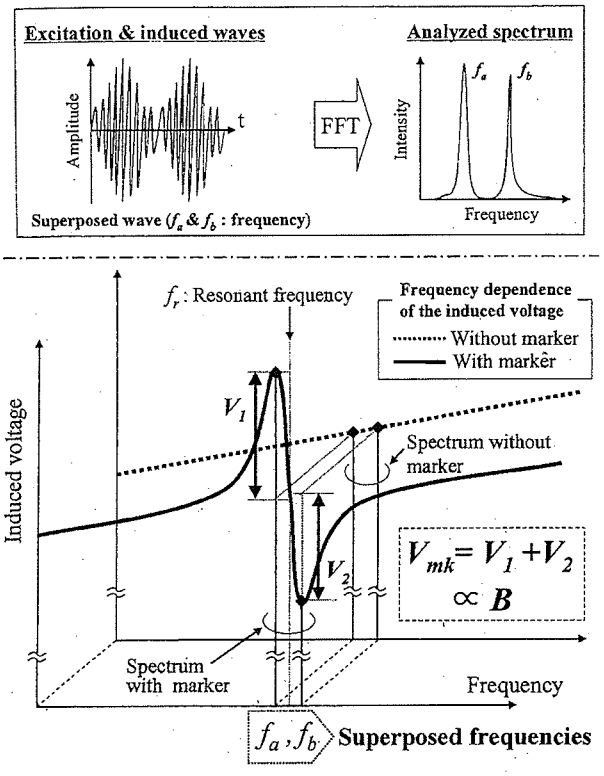

Fig. 2. Signal of LC marker acquisition technique (superposed wave excitation and FFT analysis).

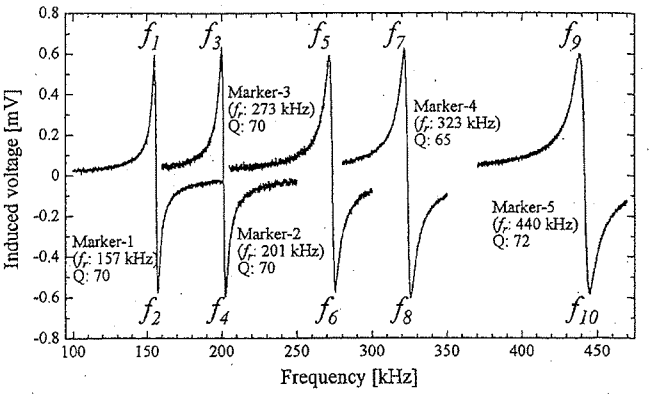

Fig. 3. Induced voltages due to excitation of five markers.

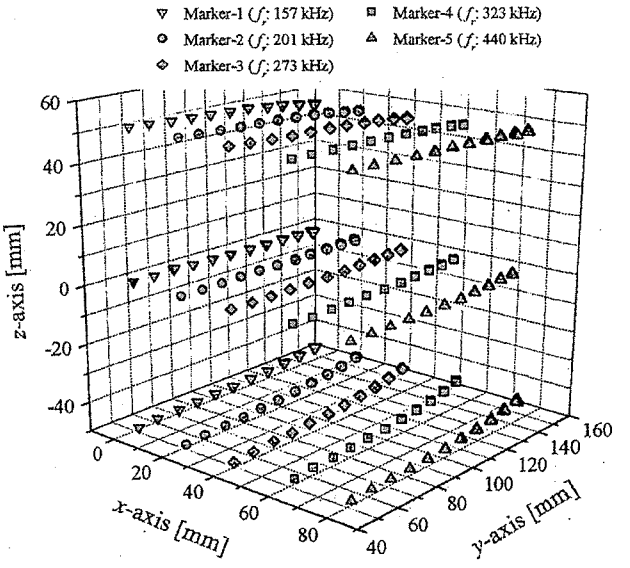

Fig. 4. Evaluation results of detected position (displayed in three dimensions).

measured with the markers. The induced voltages of the marker contributions, V_{mk}, can be obtained by subtracting as vectors the amplitude of the spectrum without the markers from the amplitude of the spectrum with the markers. The amplitudes V_{mk} measured by each pick-up coil are different from each other and proportional to the flux densities $\boldsymbol{B}$ that the markers produce at the location of the pick-up coils. The position and orientation of each marker is obtained by solving an inverse problem. However, several values (25 values in our study) of the flux density at a known location specify the magnetic flux source. To solve this problem, the generated flux density from a marker is considered to be a magnetic dipole field. Under this assumption, the position and orientation of a marker are calculated using the nonlinear method of least squares by the Gauss–Newton method [9]

$$S(\vec{p}) = \sum_{i=1}^{n} \left| \vec{B}_{\mathrm{meas}}^{(i)} - \vec{B}_{\mathrm{cal}}^{(i)}(\vec{p}) \right|^2 \rightarrow \text{Minimum} \quad (1)$$

$$\vec{B}_{\mathrm{cal}}^{(i)}(\vec{p}) = \frac{1}{4\pi\mu_0} \left\{ -\frac{\vec{M}}{r_i^3} + \frac{3(\vec{M}\cdot\vec{r}_i)\cdot\vec{r}_i}{r_i^5} \right\} \quad (2)$$

$$\vec{p} = (x, y, z, \theta, \phi, M). \quad (3)$$

Here $S(\vec{p})$ is an objective function (the least squares value), i is the coil number, n is the total number of coils, $\vec{B}_{\mathrm{meas}}^{(i)}$ is the measured flux density, $\vec{B}_{\mathrm{cal}}^{(i)}$ is the theoretical flux density that takes into account the magnetic dipole field, $\vec{p}$ represents the parameters of the marker, $\vec{M}$ is the magnetic moment, (x, y, z) is the position of the marker, and $\vec{r}$ is an ideal dipole field expressed as a function of position and orientation. As shown in Fig. 1, ϕ is the angle between the x-axis and the direction vector when the moment is projected on an xy-plane and θ is the angle between the direction of the moment and the z-axis.

Fig. 3 shows the frequency dependence of the induced voltage from the markers. Sharp signals due to LC resonance of the markers were observed and there is no influence on neighboring signals from the skirts of the signals. In practice, the superposed wave, which is composed of ten frequencies corresponding to upper and lower peaks ($f_1 - f_{10}$), shown in Fig. 3 was used for excitation.

III. Results and Discussion

The position accuracy was verified experimentally for the system. Fig. 4 shows the detected positions and Fig. 5 shows the detected orientations when the five markers were lined up in five ranks parallel to the y-axis at 20-mm intervals. The markers were swept from $y = 50$ mm to 150 mm in 10-mm steps along the y-axis in the xy-plane at $z = 50$ mm, 0 mm, -50 mm (refer

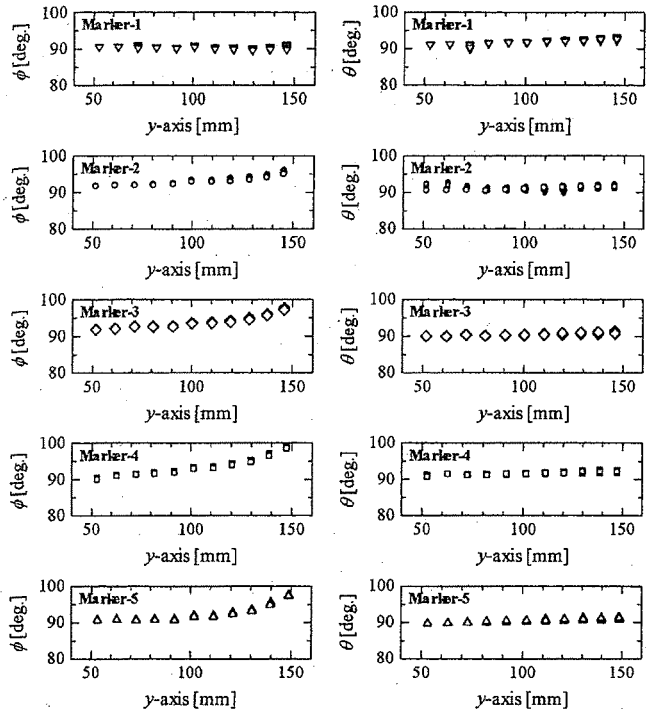

Fig. 5. Evaluation results for ϕ and θ (xy-plane at $z = 0$ mm).

to Fig. 1 for the coordinate system). As shown in Figs. 4 and 5, results can be distinguished to less than 1 mm and the position accuracy for each marker is within 2 mm. Approximately correct orientations were obtained when the markers were located up to 100 mm from the pick-up coil array. These results show that the system is capable of simultaneously capturing the motion of multi-markers wirelessly with a high accuracy. However, the detected positions were deflected toward the y-axis (the center axis of the pick-up coil array) gradually as the marker position increases over 100 mm from the pick-up coil array. Accordingly, the deviation of the attitude angle ϕ increases gradually up to about 10 degrees. A maximum positional deviation of around 6 mm was observed for markers located at (80, 150, 50), (80, 150, 0), and (80, 150, -50), whereas, as shown in Fig. 6, the intervals between adjacent markers were less than 3 mm in terms of relative position accuracy. The relative error of the measured position of all the points at intervals between adjacent markers was evaluated and expressed as an averaged value with a standard deviation. The results are as follows: 19.03 ± 0.88 mm at Mk1-2 (interval between Marker 1 and Marker 2), 18.79 ± 0.25 mm at Mk2-3, 19.88 ± 0.65 mm at Mk3-4, and 20.55 ± 0.41 mm at Mk4-5.

The increase in the detection error for large distances is thought to be due to the relation between the size and arrangement of the driving coil and the pick-up coil array, though the exact cause of these deflects is not yet clear.

IV. Conclusion

The performance of a proposed wireless magnetic motion capture system for multi-makers was evaluated for five LC resonant magnetic markers with individual resonant frequencies. The positional accuracy of the markers was found to be less than 2 mm and the approximate orientation of a marker could be determined when the marker was located within 100 mm^3, up to 100 mm from the pick-up coil array. However, the detected positions were deflected toward the y-axis (the center axis of the pick-up coil array) gradually as the distance of the marker from the pick-up coil array increased.

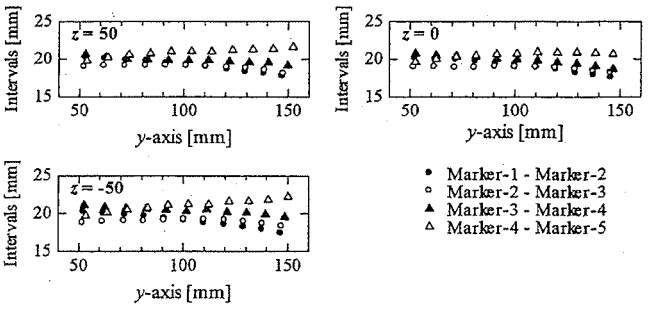

Fig. 6. Intervals between adjacent markers.

Acknowledgment

This work was supported in part by the Industrial Technology Research Grant Program in 03A47063a from the New Energy and Industrial Technology Development Organization (NEDO) of Japan, and also in part by Strategic Information and Communication R&D Promotion Programme (SCOPE) in the Ministry of Public Management, Home Affairs, Posts and Telecommunications (MPHPT).

References

[1] F. Grant and G. West, *Interpretation Theory in Applied Geophysics*. New York: McGraw-Hill, 1965, pp. 306–381.

[2] S. V. Marshall, "Vehicle detection using a magnetic field sensor," *IEEE Trans. Veh. Technol.*, vol. VT-27, pp. 65–68, 1978.

[3] W. M. Wynn, C. P. Frahm, P. J. Carroll, R. H. Clark, J. Wellhoner, and M. J. Wynn, "Advanced superconducting gradiometer/magnetometer arrays and a novel signal processing technique," *IEEE Trans. Magn.*, vol. MAG-11, pp. 701–707, 1975.

[4] F. H. Raab, E. B. Blood, T. O. Steiner, and H. R. Jones, "Magnetic position and orientation tracking system," *IEEE Trans. Aerosp. Electron. Syst.*, vol. AES-15, pp. 709–718, 1979.

[5] J. E. Mcfee and Y. Das, "Determination of the parameters of a dipole by measurement of its magnetic field," *IEEE Trans. Antennas Propag.*, vol. AP-29, pp. 282–287, 1981.

[6] J. A. Paradiso, K. Hsiao, J. Stricken, J. Lifton, and A. Adler, *IBM Syst. J.*, vol. 39, no. 3 & 4, pp. 892–914, 2000.

[7] S. Yabukami, S. Hashi, Y. Tokunaga, T. Kohno, K. I. Arai, and Y. Okazaki, "Development of a position-sensing system for a wireless magnetic marker," *J. Magn. Soc. Jpn.*, vol. 28, pp. 877–885, 2004.

[8] Y. Tokunaga, S. Hashi, S. Yabukami, T. Kohno, M. Toyoda, T. Ozawa, Y. Okazaki, and K. I. Arai, "Precision position-detecting system using an LC resonant magnetic marker," *J. Magn. Soc. Jpn.*, vol. 29, pp. 153–156, 2005.

[9] T. Nakagawa and Y. Koyanagi, *Experimental Data Analysis by the Least Square Method*. Tokyo, Japan: Univ. Tokyo Press, 1982, pp. 95–99.

Manuscript received March 13, 2006 (e-mail: hashi@cc.gifu-u.ac.jp).